Composites: Part B 55 (2013) 16–21

Contents lists available at SciVerse ScienceDirect

Composites: Part B

journal homepage: www.elsevier.com/locate/compositesb

A composite index to quantify dispersion of carbon nanotubes in polymer-based composite materials

Michael D. Haslam, Bart Raeymaekers *

Dept. of Mechanical Engineering, University of Utah, Salt Lake City, UT 84112, USA

ARTICLE INFO

Article history:
Received 23 August 2012
Received in revised form 23 March 2013
Accepted 26 May 2013
Available online 5 June 2013

Keywords:
A. Nano-structures
E. Thermosetting resin
A. Particle-reinforcement

ABSTRACT

Several methods with various levels of sophistication exist to quantify dispersion of carbon nanotubes (CNTs) in a polymer matrix, such as the ASTM D2663 standard that is often used in engineering practice. However, most methods are limited by their accuracy, complexity of implementation, and scalability. In this paper, we present a new technique and index to quantify dispersion of CNTs in a composite material. The technique is partially based on a quadrat method, and takes into account the dispersion and agglomerate size distribution of the CNTs. This index is benchmarked against the ASTM index using computer generated images and images experimentally obtained from thirty CNT composite material specimens with different CNT loading rates up to twenty volume percent. The new index is shown to be more versatile and reliable than the ASTM index. It is easily implementable in engineering practice as opposed to other more sophisticated techniques available in the literature.

1. Introduction

Carbon nanotubes (CNTs) have extraordinary mechanical properties and a high strength-to-weight ratio [1,2]. This has inspired their use as reinforcement into polymer composites [3,4]. In recent studies, the addition of CNTs to the polymer matrix has demonstrated an increase in the elastic modulus and the tensile strength of these materials [5–8]. Research has also shown that the increase in tensile strength is comparable to the predicted values from the rule of mixtures and the Halpin-Tsai equation [7]. However, when increasing the CNT loading rate, the experimentally determined tensile strength of the composite materials may fall short of the theoretically predicted value [9], oftentimes as a result of insufficient dispersion of the CNTs in the polymer matrix [10,11]. Dispersion is one of the key problems when integrating CNTs as reinforcement in composite materials [8,10,11].

Effective dispersion of CNTs is difficult to achieve due to van der Waals forces causing them to aggregate as a result of a large surface to volume ratio [12]. The energy needed to disperse the CNTs must be sufficiently high to overcome the van der Waals forces, but not so high to fracture the CNTs [13]. Several methods are used to accomplish dispersion including sonication [13,14], high speed stirring [15], the addition of a compatibilizer or surfactant [16], and melt or shear mixing [17]. Typically, a combination of these methods is employed to further enhance dispersion [18].

Quantitative measurement of dispersion is important because qualitative methods based on for instance visual observation suffer from subjective judgment and do not result in a metric that can be used to consistently compare dispersion of composite materials with the same matrix and filler constituents but with different distribution of the filler in the matrix material. Second, when a quantitative measure of dispersion exists, this measure can be correlated to constitutive properties of the composite material [19]. Several techniques exist to quantify dispersion of filler material in the matrix of the composite material. Methods based on feature size such as the relative particle size (RPS) method [20,21], and methods based on contact area [22,23] are commonly used for composites prepared by dry mixing followed by sintering or hot-pressing for ceramic and metallic composite materials.

In this paper, we focus on quantifying dispersion of CNT filler material in polymer-based composite materials. A simple method of measuring dispersion is through tensile testing of CNT polymer composite material samples [24]. Thus, the dispersion of the entire composite structure is evaluated. However, this method neglects the effect of other parameters that affect the strength of the material, such as the bond strength between the filler and matrix and orientation of the filler amongst other effects. Hence, this simple method may only be valid when comparing dispersion of different composite material samples consisting of the same filler and same matrix material. Direct measurements of CNT dispersion in a polymer can be performed by UV–visible spectroscopy [25,26], electrical conductivity [15,17], Raman spectroscopy [27], and fluorescence [28]. The spectroscopy technique is based on the bias that individual CNTs are active in the UV–visible spectrum but

* Corresponding author. Tel.: +1 801 585 7594; fax: +1 801 585 9826.
E-mail address: bart.raeymaekers@utah.edu (B. Raeymaekers).

1359-8368/$ - see front matter © 2013 Elsevier Ltd. All rights reserved.
http://dx.doi.org/10.1016/j.compositesb.2013.05.038

large aggregates are not. This method can only be applied to either an aqueous solution of CNTs or to thin films, and additionally only gives information about dispersion, not about the size of the inclusion agglomerates. Measurements by Raman spectroscopy and fluorescence face similar limitations. Transmission electron microscopy (TEM), scanning electron microscopy (SEM), and confocal optical microscopy are also used for analyzing dispersion [16,25,29,30]. TEM and SEM allow measuring the dispersion of only a very small section (1 μm) of the composite material specimen and, thus, evaluating large specimens is unrealistic. Additionally, the small section may not be representative of the entire material sample.

Microscopy does not provide a simple, quantitative measure of dispersion. Images must be processed to quantify the dispersion of CNTs. Several techniques are available to analyze these images including complex mathematical methods such as a statistical relative dispersion index based on the difference between the uniform-predicted probability of occurrence of a CNT and the observed probability [31], quantification of agglomerates using a numerical score between 1 and 10 [32], calculation of an agglomerate area ratio [33], and so-called quadrat methods adapted from ecology [34,35] or from spatial statistics [36]. Quadrat methods define dispersion by means of the standard deviation of the concentration of inclusions in sections of a microscope image of the composite material sample. The image can be divided in different sections, or one section can be translated over the image with a specific step size. Dispersion is considered to be better with lower standard deviation. The downside of quadrat methods is that the choice of quadrat mesh size can result in different judgments of dispersion. The method does not converge to a unique solution. Nevertheless, the quadrat method results in good dispersion judgment when used carefully [19,37,38]. Another limitation of the quadrat method (as well as the other methods) is that it only takes the spatial distribution (dispersion) into account, not the size distribution of the inclusion agglomerates.

Recently, Bakshi et al. [39] addressed this problem by proposing two different metrics to quantify the dispersion of CNTs in a nanocomposite; a dispersion parameter (DP) based on image analysis and a clustering parameter (CP) based on a triangulation method, thus accounting for both the spatial distribution and size distribution of the inclusions. High values of DP and CP signify good dispersion. Furthermore, Luo and Koo [40] proposed a method to quantify the dispersion and agglomeration of different shapes of particles based on a dispersion quantity measured by the free-space between the particles and an agglomeration quantity measured by the particle size. Tyson et al. [41] extended this work for cases where the particles have a uniform shape, or touch each other. Finally, an ASTM standard and an ASTM index exist to analyze and quantify dispersion of carbon in a compound [42]. However, the ASTM index is not as sophisticated as the previously described methods, and seems to sometimes result in counter-intuitive results, as will be shown in Section 3 of this paper. Most of these techniques to quantify dispersion are either limited by the size of samples that can be evaluated, or by their ease of implementation due to use of complex mathematics and expensive instrumentation. As a result, in engineering practice, microscopy images are often only used for qualitative observation of dispersion [8,13], or simple techniques such as the ASTM index are employed.

An attractive quantitative measure of dispersion must be intuitive, simple, and capable of quantifying dispersion for any kind of composite material [19]. Additionally, it should be non-subjective and be implementable in engineering practice. Hence, in this paper we present a new algorithm and index, referred to here as the composite index, which allows quantifying dispersion more reliably than the ASTM index without adding complexity. The index is partially based on a quadrat method but accounts for both the dispersion and size distribution of the inclusions. The effectiveness of this method is evaluated and compared to the ASTM standard, using specific benchmark test images and actual microscopy images from CNT-polymer composite materials.

2. Dispersion index

2.1. ASTM Index

The ASTM D2663 standard [30] describes a technique and index for quantifying the dispersion of carbon in a compound. It encompasses three methods, of which the microscopy agglomerate count method (Method B) is commonly used in engineering practice to quantify dispersion of CNT filler in the polymer matrix of composite materials, see for instance [17,43]. This standard is based on a microscope image of the CNT polymer composite, and requires dividing this image into nine equal-sized sections (Fig. 1). Each of these nine sections is further divided into 10,000 squares that, under proper magnification, are 10×10 μm in size for a total of 90,000 squares. A count of all squares that are at least half full of carbon is performed for only five of the nine sections. Fig. 1 displays the four sections that are eliminated in gray. This count is divided by five to obtain an average over the five sections, and is assigned the variable U. The ASTM dispersion index D is calculated as

$$D = 100 - \frac{SU}{L} \tag{1}$$

where L is the volume percentage (0–100) of carbon in the polymer composite and S is the swelling factor (only used for rubber compounds and considered equal to 1 here). The index ranges between 0 and 100, with 100 indicating perfect dispersion. Negative values for D can result from Eq. (1) but are set to 0 by definition. The ASTM index does not consider how closely packed the carbon is and does not compare carbon content between the nine sections of the image, for instance to detect carbon agglomerates. The total carbon content is averaged over the entire image.

2.2. Composite index

The composite index, *compIndex*, consists of two parts: the dispersion distribution index *dIndex* and the size distribution index *sIndex*. This is based on the notion that quantifying dispersion should account for the spatial location of the CNTs (how well

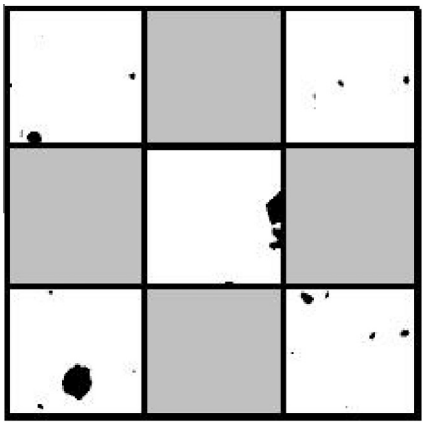

Fig. 1. Illustration of the ASTM standard for quantifying the dispersion of carbon in a compound, showing an image of carbon (black) in a polymer (white), covering an area of 3 by 3 mm. A grid divides the image in nine sections of which only five (non-gray) are considered in the dispersion evaluation.

spread out the carbon is) but also the size of the clusters of CNTs (how large the carbon agglomerates are) [44]. Each part contains two components; one relates to the shape of the distribution and one relates to the range of the distribution.

The dispersion distribution index is determined using a quadrat method based on a 3×4 grid as shown in Fig. 2, chosen to coincide with the aspect ratio of standard photo images. All image sections are included in the calculation of the index, thus accounting for the entire image area. As with all quadrat methods, the results depend on the ratio of quadrat to particle size, a problem this technique does not solve. However, the method was tested and found to be reliable when comparing different dispersion results for 0–20 vol% CNT loading rates. It was also found that for these loading rates, the quadrat to particle size ratio must exceed 1000 to obtain reliable results.

The dispersion distribution index is calculated as

$$dIndex = \frac{1}{2}\left[1 - \frac{s(b)}{0.5222} + \frac{\bar{b}}{\max(b)}\right] \tag{2}$$

where b is the set of carbon content values observed for each of the twelve sections of the image, expressed as a percentage. $s(b)$ is the standard deviation of b, and $\bar{b}$ is the arithmetic average of b. The constant 0.5222 is the largest possible standard deviation for twelve numbers that range between 0 and 1, namely the set of six zeros and six ones. Eq. (2) accounts for the shape of the dispersion distribution by means of the standard deviation, $s(b)$. If $s(b)$ increases and approaches 0.5222, which reflects increased variation in the carbon content per section, the *dIndex* is reduced to account for poorer dispersion. The range of the distribution is considered by means of the ratio of the average carbon concentration to the maximum carbon concentration in any image section. A large difference between $\bar{b}$ and $\max(b)$ will result in a small fraction $\bar{b}/\max(b)$, again reducing the *dIndex* to reflect poor dispersion. Although they are not completely independent, both the $s(b)/0.5222$ and the $\bar{b}/\max(b)$ terms are needed in Eq. (2). Indeed, one can imagine separate cases in which $s(b)/0.5222$ remains constant but $\bar{b}/\max(b)$ remains constant and vice versa. Thus, both terms are needed to ensure that all changes in dispersion result in a change in the *dIndex*. The outcome of the *dIndex* is contained between 0 and 1, with 1 indicating perfect dispersion of the carbon in the image, however, not taking into account the size of the carbon agglomerates.

It seems desirable to perform the calculation of the size distribution index without a grid, since large particle agglomerates are likely to cross grid boundaries. The area of each particle agglomerate a_i in an image is determined by counting the number of pixels occupied by each particle agglomerate, and *sIndex* is then computed as

$$sIndex = \frac{1}{2}\left[\frac{l}{N} + 1 - \frac{\max(a)}{\sum_{i=1}^{N} a_i}\right] \tag{3}$$

with a the set of all particle agglomerate sizes in the image being analyzed. N is the total number of particle agglomerates and l is the number of particle agglomerates whose area is less than a threshold of 100 pixels. The threshold was selected to be independent of the vol% CNTs in the sample, to make the resulting index independent of the expected carbon concentration. The value of 100 pixels is the maximum particle agglomerate size obtained for images with randomly generated dispersion up to 20 vol% (4 wt%). Thus, when observing an agglomerate of carbon covering more than 100 pixels it indicates less than perfect dispersion. On the other hand, good dispersion will result in a ratio of l/N that is close to one, thus increasing *sIndex*. The index accounts for the size distribution with the threshold count, and the range of the size distribution by means of the ratio of the maximum area to the total area. For instance, a single large cluster of carbon would penalize the *sIndex* because the fraction $\max(a)/\sum_{i=1}^{N} a_i$ is large. The *sIndex* ranges between 0 and 1, with 1 being assigned to an image with no observed particles, indicating that the agglomerates of CNTs are too small to be detected in the image, thus indicating good dispersion.

The composite index *compIndex* is finally calculated as the arithmetic average of the *dIndex* and the *sIndex*, implying that equal importance is attributed to both spatial dispersion and size dispersion of the carbon in the analyzed microscope image. The two separate indexes should still be reported in conjuction with the *compIndex* to better characterize the dispersion.

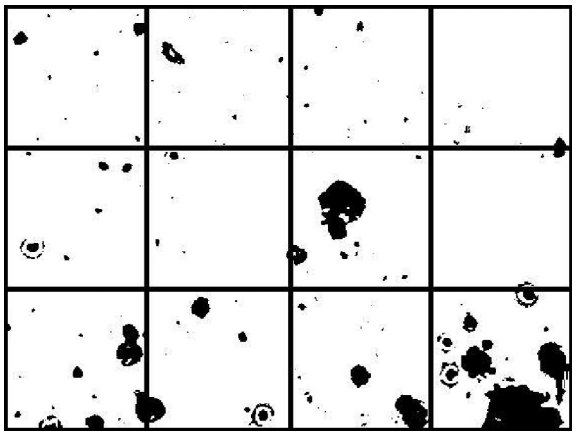

Fig. 2. Illustration of the 3×4 grid, covering a 6.5 by 4.9 mm area, used in the dispersion distribution index calculation.

3. Results and discussion

The new *compIndex* is compared to the ASTM standard using a benchmark test and a sample test. The benchmark test utilizes three computer generated images shown in Fig. 3, with a 5 vol% CNT loading rate. Fig. 3a is a random distribution of carbon, Fig. 3b and c are identical carbon aggregates in different locations of the image. The sample test utilizes three images, shown in Fig. 4, obtained from polymer composite material samples with randomly dispersed CNTs. The samples consist of a thermoset resin matrix with multi-walled CNTs with a diameter of 50–80 nm, and a length of 10–20 μm. The CNT-polymer composite material sample is loaded until fracture in a uni-axial tensile test, and a picture of the fracture surface is obtained using an optical microscope with a digital camera. The picture is converted to a binary image using a luminance cutoff of 0.2, resulting in an image that shows the CNTs in black and the polymer in white. Since the ASTM index requires a 1:1 image aspect ratio as opposed to the 3:4 ratio for the *compIndex*, the center portion of the latter was used to satisfy the requirements of the former. Fig. 4a–c represent CNT loading rates of 2.9, 5.6, and 10.7 vol%, respectively.

The resulting dispersion indexes obtained from the benchmark and sample images, with both the newly proposed *compIndex* and the existing ASTM index are shown in Table 1. Both indexes show almost perfect dispersion results for benchmark (a), as expected for an image with randomly generated black pixels. However, the two indexes differ significantly in their handling of benchmarks (b and c). Even though the samples contain an equal size and dispersion distribution of carbon, the ASTM index yields opposite results for benchmark (b) = 0 and (c) = 100, because in the case of benchmark (b) all carbon is concentrated in a section of the image that is not considered in the index (gray colored in Fig. 1). The *compIndex* handles these benchmark images more consistently, yielding nearly identical results of approximately 0.26, which matches the visually

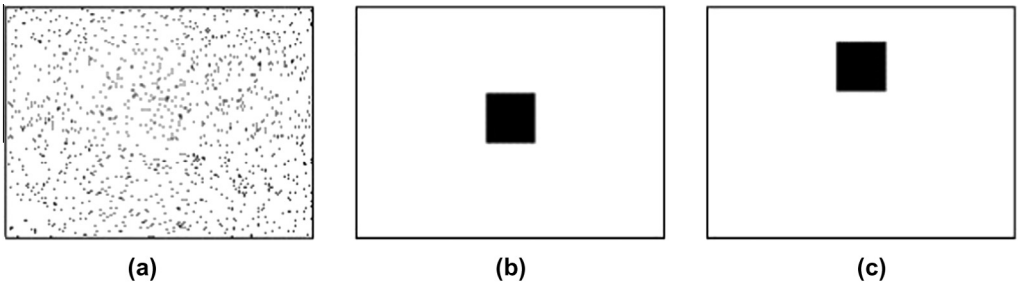

Fig. 3. Benchmark images used to compare the ASTM index to the new composite index; (a) a random computer generated 5 vol% sample, (b and c) show two variations of a 5 vol% sample in one aggregate.

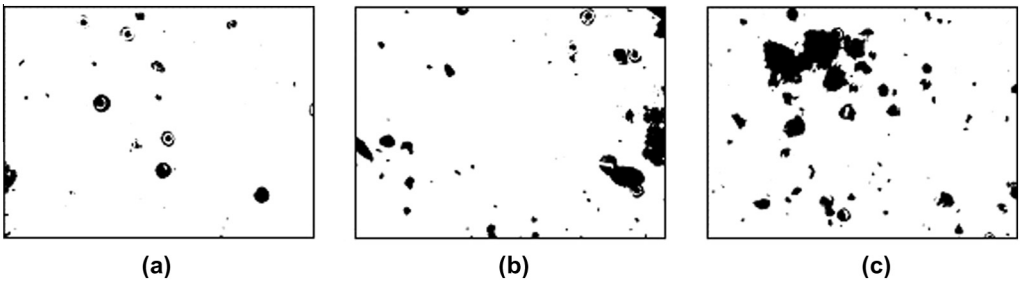

Fig. 4. Sample images used to compare the ASTM index to the new composite index; (a) 2.9, (b) 5.6, and (c) 10.7 vol%, corresponding to 0.5, 1, and 2 wt%, respectively.

Table 1
Dispersion index results from the ASTM index and the *compIndex* (*dIndex* and *sIndex*) for six test images.

Image	ASTM index (*D*)	*dIndex*	*sIndex*	*CompIndex*
Benchmark (a)	100.0	0.994	0.999	0.997
Benchmark (b)	0.0	0.511	0.000	0.255
Benchmark (c)	100.0	0.533	0.000	0.267
Sample (a)	54.4	0.677	0.717	0.697
Sample (b)	69.6	0.562	0.553	0.557
Sample (c)	0.0	0.479	0.572	0.526

observed dispersion. Also, the *sIndex* = 0 for benchmark (a and b) recognizing that all carbon is lumped in one agglomerate, which cannot be identified with the ASTM index. This is an improvement over the ASTM index and exploits the limitation behind sectioning the image using a grid.

The results from the sample images also illustrate the limitations of the ASTM index. Visually, the dispersion of the samples ranks (a) (Fig. 4a) most dispersed and (c) (Fig. 4c) least dispersed. While *the compIndex* agrees with qualitative intuition based on visual observation, the ASTM standard does not. It ranks sample (b) (Fig. 4b) as most dispersed. The ASTM index does not consider how closely packed the carbon is and, thus, the large cluster on the right in sample (b) is averaged over the entire image, yielding a higher dispersion index than it deserves based on visual observation. The ASTM index ranks sample (c) (Fig. 4c) last with $D = 0$. This value is equivalent to the result found for benchmark (b) (Fig. 3b) where all the carbon is concentrated in one location. Sample (c) clearly displays better dispersion than benchmark (b) but the ASTM index does not distinguish between both cases. Contrary to the ASTM index, the *compIndex* is able to correctly handle dispersions that are poor (benchmark (b)) and near perfect (benchmark (a)) without losing its ability to quantify the dispersions of actual parts (samples (a–c)).

Both indexes are used to quantify the dispersion of 30 CNT composite material samples that have loading rates ranging between 0.88 vol% (0.15 wt%) and 10 vol% (2.0 wt%), using the method described above. Six samples are analyzed for each CNT loading rate. The multi-walled CNTs are dispersed in the thermoset resin matrix using bath sonication at 42 kHz and 35 Watts for 380 s (Blazer Products Inc., 3800-A), prior to cross-linking. Sonication is a simple, convenient, and economical way of dispersing CNTs [18]. Even though this technique has been found to be inconsistent for the dispersion of CNTs in polymers [24], the intent of this study is to quantify the dispersion, not to obtain perfect dispersion.

Fig. 5 shows the average dispersion index versus the CNT loading rate with errorbars that represent one standard deviation, calculated from the six samples evaluated for each CNT loading rate. The ASTM index *D* is divided by 100 to map it on a 0 to 1 scale and allow direct comparison to the *compIndex*. The ASTM index ranks all images significantly less dispersed than the *compIndex* because it finds a value of $D = 0$ for 22 out of 30 samples. This indicates that

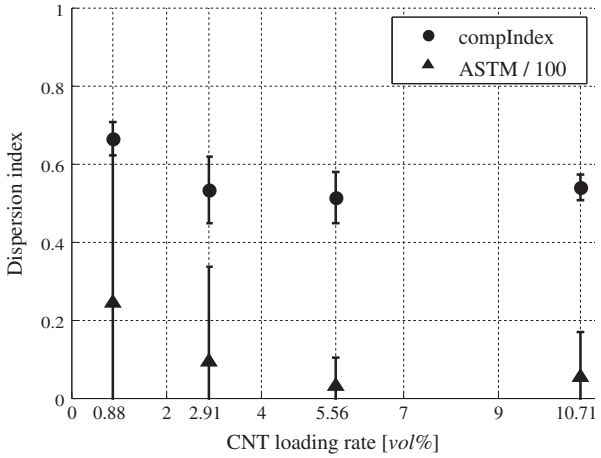

Fig. 5. Comparison of the ASTM dispersion index and the compIndex versus loading rate for 30 CNT composite material samples.

the ASTM index is not well-suited to measure a wide range of dispersion results. The ASTM index also does not compare between samples. All the evaluated samples are fabricated using the same technique and protocol, yet the standard deviation of the resulting index value is as high as 0.41 for the 0.88 vol% (0.15 wt%) case. In fact, for this case, the ASTM index finds one sample with $D = 100$ and several samples with $D = 0$. This is a significant difference from the *compIndex*, which does not rank any samples in our experiments below 0.39 or above 0.74, and the largest standard deviation of the *compIndex* for any CNT loading rate is found to be 0.09. Despite these large differences, the average values of the two indexes display the same trend when evaluating the dispersion index as a function of CNT loading rate (Fig. 5). Thus, although the dispersion results for individual samples may differ significantly, the *compIndex* and the ASTM index yield the same qualitative results.

4. Conclusion

Quantifying the dispersion of CNTs in a polymer matrix involves two primary factors; the dispersion distribution of particles (how well spread out the carbon is) and the size distribution of particles (how large the carbon agglomerates are) throughout the sample. Both of these factors must be measured to effectively determine the dispersion of CNTs in a composite material. The ASTM index, which is commonly used in engineering practice, displays several limitations to measuring these two factors. First, it does not consider the distribution of carbon over the entire sample, because it does not compare the amount of carbon between different sections of the image, but calculates an average over all sections. Second, it does not take into account the size of carbon particles or agglomerates. Finally, the index arbitrarily eliminates four of the nine sections it defines, the inclusion of which was shown to substantially alter the resulting index.

The *compIndex* is based on using a two part evaluation that includes the dispersion distribution (*dIndex*) and the size distribution of carbon (*sIndex*). The measurement results thus found were accurate and consistent from sample to sample as opposed to evaluating the sample samples with the ASTM index. While both indexes obtain the same qualitative result and are easy to implement using computer algorithms, the *compIndex* is an improvement because it provides more consistent results that match the visual observation of dispersion. It adds sophistication without adding complexity.

Finally, while myriad techniques with various level of sophistication exist to quantify dispersion, the *compIndex* offers an effective, easily implementable alternative to qualitative assessment or less sophisticated methods such as the ASTM index.

References

[1] Demczyk B, Wang Y, Cumings J, Hetman M, Han W, Zettl A, et al. Direct mechanical measurement of the tensile strength and elastic modulus of multiwalled carbon nanotubes. Mater Sci Eng A 2002;334:173–8.
[2] Li C. Elastic moduli of multi-walled carbon nanotubes and the effect of van der Waals forces. Compos Sci Technol 2003;63:1517–24.
[3] Lau AKT, Hui D. The revolutionary creation of new advanced materials—carbon nanotube composites. Composites B 2002;33:263–77.
[4] Breuer O, Sundararaj U. Big returns from small fibers: a review of polymer/carbon nanotube composites. Polym Compos 2004;25:630–45.
[5] Xu X, Thwe MM, Shearwood C, Liao K. Mechanical properties and interfacial characteristics of carbon-nanotube-reinforced epoxy thin films. Appl Phys Lett 2002;81:2833–5.
[6] Bai JB. Evidence of the reinforcement role of chemical vapour deposition multi-walled carbon nanotubes in a polymer matrix. Carbon 2003;41:1325–8.
[7] Coleman J, Khan U, Blau W, Gunko Y. Small but strong: a review of the mechanical properties of carbon nanotube–polymer composites. Carbon 2006;44:1624–52.
[8] Chou T-W, Gao L, Thostenson ET, Zhang Z, Byun J-H. An assessment of the science and technology of carbon nanotube-based fibers and composites. Compos Sci Technol 2010;70:1–19.
[9] Zhu J, Peng H, Rodriguez-Macias F, Margrave JL, Khabashesku VN, Imam AM, et al. Reinforcing epoxy polymer composites through covalent integration of functionalized nanotubes. Adv Funct Mater 2004;14:643–8.
[10] Ajayan PM, Schadler LS, Giannaris C, Rubio A. Single-walled carbon nanotube–polymer composites: strength and weakness. Adv Mater 2000;12:750–3.
[11] Esawi AMK, Farag MM. Carbon nanotube reinforced composites: potential and current challenges. Mater Des 2007;28:2394–401.
[12] Qian D, Dickey EC, Andrews R, Rantell T. Load transfer and deformation mechanisms in carbon nanotube–polystyrene composites. Appl Phys Lett 2000;76:2868–70.
[13] Huang YY, Terentjev EM. Dispersion of carbon nanotubes: mixing, sonication, stabilization, and composite properties. Polymers 2012;4:275–95.
[14] Bandyopadhyaya R, Nativ-Roth E, Regev O, Yerushalmi-Rozen R. Stabilization of individual carbon nanotubes in aqueous solutions. Nano Lett 2002;2:25–8.
[15] Sandler J, Shaffer M, Prasse T, Bauhofer W, Schulte K, Windle A. Development of a dispersion process for carbon nanotubes in an epoxy matrix and the resulting electrical properties. Polymer 1999;40:5967–71.
[16] Rastogi R, Kaushal R, Tripathi SK, Sharma AL, Kaur I, Bharadwaj LM. Comparative study of carbon nanotube dispersion using surfactants. J Colloid Interface Sci 2008;328:421–8.
[17] Pötschke P, Bhattacharyya AR, Janke A. Melt mixing of polycarbonate with multiwalled carbon nanotubes: microscopic studies on the state of dispersion. Eur Polym J 2004;40:137–48.
[18] Xie X, Mai Y, Zhou X. Dispersion and alignment of carbon nanotubes in polymer matrix: a review. Mater Sci Eng R 2005;49:89–112.
[19] Yazdanbakhsh A, Grasly Z, Tyson B, Abu Al-Rub RK. Dispersion quantification of inclusions in composites. Compos Part A: Sci 2011;42:75–83.
[20] Bhanu Prasad VV, Bhat BVR, Ramakrishnan P, Mahajan YR. Clustering probability maps for private metal matrix composites. Scr Mater 2000;43(9):835–40.
[21] Slipenyuk A, Kuprin V, Milman Y, Spowart JE, Miracle DB. The effect of matrix to reinforcement particle size ratio (PSR) on the microstructure and mechanical properties of P/M processed AlCuMn/SiCp MMC. Mater Sci Eng, A 2004;381(1–2):165–70.
[22] Gurland J. In: DeHoff RT, Rhine FN, editors. Quantitative microscopy. Berlin: Springer; 1968.
[23] Jang BZ, Chang YS. Assessment of particle size distribution and spatial distribution of rubbery phase in a toughened plastic. In: Particle size distribution. Washington, DC: American Chemical Society; 1987. p. 30–45.
[24] Liao Y-H, Marietta-Tondin O, Liang Z, Zhang C, Wang B. Investigation of the dispersion process of SWNTs/SC-15 epoxy resin nanocomposites. Mater Sci Eng A 2004;385:175–81.
[25] Yu J, Grossiord N, Koning CE, Loos J. Controlling the dispersion of multi-wall carbon nanotubes in aqueous surfactant solution. Carbon 2007;45:618–23.
[26] Georgakilas V, Bourlinos A, Gournis D, Tsoufis T, Trapalis C, Mateo-Alonso A, et al. Multipurpose organically modified carbon nanotubes: from functionalization to nanotube composites. J Am Chem Soc 2008;130:8733–40.
[27] Izard N, Riehl D, Anglaret E. Exfoliation of single-wall carbon nanotubes in aqueous surfactant suspensions: a Raman study. Phys Rev B 2005;71:195417.
[28] O'connell MJ, Bachilo SM, Huffman CB, Moore VC, Strano MS, Haroz EH, et al. Band gap fluorescence from individual single-walled carbon nanotubes. Science 2002;297:593–6.
[29] Eckel DF, Balogh MP, Fasulo PD, Rodgers WR. Assessing organo-clay dispersion in polymer nanocomposites. J Appl Polym Sci 2004;93(3):1110–7.
[30] Xie S, Harkin-Jones E, Shen Y, Hornsby P, McAfee M, McNally T, et al. Quantitative characterization of clay dispersion in polypropylene–clay nanocomposites by combined transmission electron microscopy and optical microscopy. Mater Lett 2010;64(2):185–8.
[31] Kashiwagi T, Fagan J, Douglas JF, Yamamoto K, Heckert AN, Leigh SD, et al. Relationship between dispersion metric and properties of PMMA/SWNT nanocomposites. Polymer 2007;48:4855–66.
[32] Andrews R, Jacques D, Minot M, Rantell T. Fabrication of carbon multiwall nanotube/polymer composites by shear mixing. Macromol Mater Eng 2002;287:395–403.
[33] Kasaliwal GR, Pegel S, Göldel A, Pötschke P, Heinrich G. Analysis of agglomerate dispersion mechanisms of multiwalled carbon nanotubes during melt mixing in polycarbonate. Polymer 2010;51:2708–20.
[34] Kim D, Lee JS, Barry CMF, Mead JL. Microscopic measurement of the degree of mixing for nanoparticles in polymer nanocomposites by TEM images. Microsc Res Tech 2007;70:539–46.
[35] Gleason HA. Some applications of the quadrat method. Bull Torrey Bot Club 1920;47(1):21–33.
[36] Pegel S, Pötschke P, Villmow T, Stoyan D, Heinrich G. Spatial statistics of carbon nanotube polymer composites. Polymer 2009;50:2123–32.
[37] Fan LT, Chen Y-M, Lai FS. Recent developments in solids mixing. Powder Technol 1990;61(3):255–87.
[38] Rhodes MJ. Introduction to particle technology. New York: John Wiley & sons; 1998.
[39] Bakshi SR, Batista RG, Agarwal A. Quantification of carbon nanotube distribution and property correlation in nanocomposites. Compos Part A: Appl Sci Manuf 2009;40(8):1311–8.
[40] Luo ZP, Koo JH. Quantifying the dispersion of mixture microstructures. J Microsc – Oxford 2007;225(2):118–25.
[41] Tyson BM, Abu Al-Rub RK, Yazdankbakhsh A, Grasley Z. A quantitative method for analyzing the dispersion and agglomeration of nano-particles in composite materials. Compos Part B: Eng 2011;42(6):1395–403.

[42] ASTM D2663 standard, method B.
[43] Krause B, Pötschke P, Häußler L. Influence of small scale melt mixing conditions on electrical resistivity of carbon nanotube–polyamide composites. Compos Sci Technol 2009;69:1505–15.
[44] Kissinger-Kane MC, Investigation and characterization of the dispersion of nanoparticles in a polymer matrix by scattering techniques, PhD thesis. University of Florida; 2007.